Electronic Supplementary Material (ESI) for Nanoscale.

Supporting Information

Nano-assembly of ruthenium(II) photosensitizers for endogenous glutathione depletion and enhanced two-photon photodynamic therapy

Libing Ke,[a], Fangmian Wei,[a] Xinxing Liao,[a] Thomas W. Rees,[a] Shi Kuang,[a] Zhou Liu,[a], Yu Chen,[a] Liangnian Ji,[a] and Hui Chao*,[a]

[a] *MOE Key Laboratory of Bioinorganic and Synthetic Chemistry, School of Chemistry, Sun Yat-Sen University, Guangzhou, 510275, P. R. China. E-mail: ceschh@mail.sysu.edu.cn,*

Materials and general measurements

Unless otherwise specified, all reagents were purchased from commercial sources and used without further purification. $RuCl_3 \cdot H_2O$, 1,8-dibromooctane, potassium thioacetate, 3-(4,5-dimethylthiazol-2-yl)-2,5-diphenyltetrazolium bromide (MTT), 2,7-dichlorodihydro-fluorescein diacetate (DCFH-DA), 2,2,6,6-tetramethylpiperidine (TEMP), 1,3-diphenyliso-benzofuran (DPBF), the Annexin V-FITC apoptosis assay kit, Lyso-tracker green, Mito-tracker green and the live/dead cell imaging kit were purchased from Thermo Fisher Scientific. [2,2'-bipyridine]-4,4'-diol, $[Ru(bpy)_2]Cl_2$ and $[Ru(dpip)_2]Cl_2$ were prepared according to corresponding literature methods.[1-2]

^1H NMR spectra were performed on a nuclear magnetic resonance spectrometer (Bruker Avance III, 400 MHz), tetramethylsilane (TMS) was used as the shift reference. Electrospray ionization mass spectra (ESI-MS) were obtained by an LCQ system (Finnigan MAT, USA). Microanalyses (C, H and N) were determined by elemental analyzer (Elementar, Vario EL cube). The absorption spectra and emission spectra were recorded using a Perkin-Elmer Lambda 850 UV/Vis spectrometer and Perkin-Elmer LS 55 luminescence spectrometer respectively. Infrared spectra were obtained on a Bruker BECTOR22 spectrometer in KBr pellets over a range of 400-4000 cm^{-1}.TEM images and bio-TEM images were recorded in a 120kV transmission electron microscopy (JEOL, JEM-1400 Plus, Japan). High-resolution TEM images, HADDF-STEM and elemental mapping images were obtained by Spherical aberration corrected transmission electron microscope (JEM-ARM200P, Japan). Inductively coupled plasma mass spectrometry (ICP-MS, Thermo Elemental Co., Ltd.) was used to determine the content of ruthenium (^{101}Ru). Dynamic light scattering and zeta potential experiments were performed using dynamic laser light scattering equipment (BI-PALS03030131, Brookhaven Inst. Corp.). Confocal microscopy images were recorded on LSM 810 NLO *Zeiss) microscope. Flow Cytometry was performed on a BD FACS Canto II flow cytometer. Milli-Q water was obtained from a Milli-Q system of Millipore Company (Boston, MA, USA). The electron spin-resonance spectroscopy (EPR) spectra were measured using a Bruker e-scan EPR spectrometer. *In vivo* images were recorded on an IVIS Lumina XRMS Series III imaging system (PerkinElmer).

Synthesis and characterization

Synthesis of 4,4'-bis((8-bromooctyl)oxy)-2,2'-bipyridine (bpy-2Br). [2,2'-bipyridine]-4,4'-diol (1.00 g, 5.30 mmol, 1 eq), 1,8-dibromooctane (8.65 g, 31.8 mmol, 6 eq) and K_2CO_3 (4.40 g, 31.8 mmol, 6 eq) were added into acetone (50 mL) and refluxed for 6 h. After cooling to room temperature, the solvent was removed under reduced pressure. The crude product was purified by column chromatography on silica (100-200 mesh, CH_2Cl_2:ethyl acetate, 25:1) to yield a white solid (1.88 g, 3.29 mmol, 62%). Anal. Calcd. for $C_{26}H_{38}Br_2N_2O_2$ (%): C, 54.75; H, 6.72; N, 4.91. Found: C, 54.63; H, 6.91; N, 4.79. ESI-MS (CH_3OH) m/z: 571.27 $[L+H]^+$. ^1H NMR (400 MHz, $CDCl_3$) δ 8.46 (d, *J* = 3.9 Hz, 2H), 7.98 (s, 2H), 6.84 (d, *J* = 3.9 Hz, 2H), 4.14 (t, *J* = 4.0 Hz, 4H), 3.46 (t, *J* = 4.1 Hz, 4H), 1.91-1.79 (m, 8H), 1.50-1.43 (m, 8H), 1.39-1.30 (m, 8H).

Synthesis of S,S'-(([2,2'-bipyridine]-4,4'-diylbis(oxy))bis(octane-8,1-diyl)) diethanethioate (bpy-2SAc). To a stirred solution of **bpy-2Br** (600 mg, 1.00 mmol, 1 eq) in acetone (50 mL), potassium thioacetate (720 mg, 6.00 mmol, 6 eq) was added. The reaction was refluxed under argon for 3 h. The crude product was collected by filtration and purified by column chromatography on silica (100-200 mesh, CH_2Cl_2:ethyl acetate, 100:3) to yield a pale-yellow solid (310 mg, 550 μmol, 55%). Anal. Calcd. for $C_{30}H_{44}N_2O_4S_2$ (%): C, 64.25; H, 7.91; N, 5.00. Found: C, 64.08; H, 8.11; N, 4.85. ESI-MS (CH_3OH) m/z: 561.64 $[L+H]^+$.^1H NMR (400 MHz, $CDCl_3$) δ 8.47 (d, *J* = 3.9 Hz,

2H), 7.98 (s, 2H), 6.85 (d, *J* = 3.9 Hz, 2H), 4.14 (t, *J* = 4.0 Hz, 4H), 2.88 (t, *J* = 4.1 Hz, 4H), 2.33 (s, 6H), 1.86-1.79 (m, 4H), 1.60-1.59 (m, 4H), 1.57-1.55 (m, 4H), 1.48-1.36 (m, 12H).

Synthesis of 8,8'-([2,2'-bipyridine]-4,4'-diylbis(oxy))bis(octane-1-thiol) (bpy-2SH). To a solution of **bpy-2SAc** (300 mg, 0.5 mmol, 1 eq) in CH_2Cl_2, a solution of KOH (300 g) in MeOH was added and stirred for 60 min. Then another solution of acetic acid (1.5 mL) in CH_2Cl_2 (10 mL) was added dropwise and subsequently stirred for 30 min. The reaction was terminated by addition of H_2O (20 mL) under vigorous stirring. The crude product in organic layer was washed three times with H_2O (10 mL), then collected and purified by column chromatography on silica (100-200 mesh, CH_2Cl_2:CH_3OH, 50:3) to give a white solid (98.0 mg, 210 μmol, 41%). Anal. Calcd. for $C_{26}H_{40}N_2O_2S_2$ (%): C, 65.50; H, 8.46; N, 5.88. Found: C, 65.36; H, 8.62; N, 5.73. ESI-MS (CH_3OH) m/z: 477.48 $[L+H]^+$.^{1}H NMR (400 MHz, $CDCl_3$) 8.46 (d, *J* = 4.1 Hz, 2H), 7.96 (s, 2H), 6.83 (d, *J* = 3.9 Hz, 2H), 4.12 (t, *J* = 4.1 Hz, 4H), 2.63 (t, *J* = 3.9 Hz, 4H), 1.84-1.71 (m, 4H), 1.63-1.62 (m, 4H), 1.60-1.59 (m, 4H), 1.47-1.36 (m, 12H).

Synthesis of [Ru(bpy)2(bpy-2SH)]Cl_2 (Ru1). Bpy-2SH (50.0 mg, 100 μmol, 1 eq) and $Ru(bpy)_2Cl_2$ (51.0 mg, 110 μmol, 1.1 eq) were dissolved in EtOH/H_2O (30 mL, 9:1, v/v), and the solution was refluxed overnight under argon. Solvent was removed under reduced pressure and the crude product was purified by column chromatography on neutral aluminum oxide (100-200 mesh, CH_2Cl_2:CH_3OH, 10:1) to yield a red solid (75.1 mg, 80.0 μmol, 78%). Anal. Calcd. for $C_{46}H_{56}Cl_2N_6O_2S_2Ru$: C, 57.49; H, 5.87; N, 8.74. Found: C, 57.03; H, 5.97; N, 8.61. ESI-MS (CH_3OH) m/z: 445.22 $[M-2Cl]^{2+}$. ^{1}H NMR (400 MHz, CD_3OD) δ 8.72 (d, *J* = 4.1 Hz, 4H), 8.28 (s, 2H), 8.12 (q, *J* = 4.1 Hz, 4.0 Hz, 4H), 7.95 (d, *J* = 3.9 Hz, 2H), 7.83 (d, *J* = 3.9 Hz, 2H), 7.53-7.46 (m, 6H), 7.08 (d, *J* = 4.1 Hz, 2H), 4.27 (t, *J* = 4.1 Hz, 4H), 2.67 (t, *J* = 3.9 Hz, 4H), 1.87-1.85 (m, 4H), 1.79-1.76 (m, 4H), 1.60-1.39 (m, 4H), 1.31-1.27 (m, 12H).

Synthesis of [Ru(dpip)2(bpy-2SH)]Cl_2 (Ru2). Ru2 was synthesized and purified *via* the same method used for **Ru1** as described above, with the exception that $Ru(bpy)_2Cl_2$ was replaced by $Ru(dpip)_2Cl_2$ (100 mg, 70.0 μmol, 72%). Anal. Calcd. for $C_{76}H_{72}Cl_2N_{10}O_2S_2Ru$: C, 65.50; H, 5.21; N, 10.05. Found: C, 65.02; H, 5.31; N, 9.93. ESI-MS (CH_3OH) m/z: 660.89 $[M-2Cl]^{2+}$. ^{1}H NMR (400 MHz, CD_3OD) δ 9.30 (m, 2H), 8.43-8.29 (m, 4H), 8.06 (d, *J* = 4.1 Hz, 2H), 7.79-7.73 (m, 12H), 7.70-7.65 (m, 8H), 7.51-7.47 (m, 4H), 7.45-7.42 (m, 4H), 7.00-6.94 (m, 2H), 4.24 (t, *J* = 4.1 Hz, 4H), 2.50 (t, *J* = 4.1 Hz, 4H), 1.87-1.80 (m, 4H), 1.62-4.57 (m, 4H), 1.52-1.48 (m, 4H), 1.41-1.37 (m, 12H).

Synthesis of RuS NPs and HA@RuS NPs

Ru1 or **Ru2** (10 mg) were dissolved in DMSO (3 mL). I_2 in DMSO (100 μL, 1 mol/L) was added dropwise under vigorous stirring for 6 h. Then the mixture was diluted with EtOH (10 mL) and centrifuged at 6000 rpm for 15 min. The precipitate was washed with EtOH three times and resuspended in deionized water before undergoing dialysis (MWCO=3000) with saline solution for purification. **RuS NPs** were obtained by lyophilization.

For **HA@RuS2 NPs**, sodium hyaluronic acid (50 mg) was dissolved in deionized water (20 mL). Then **RuS2 NPs** solution in EtOH (1 mL, 2 mg/mL) was added under vigorous stirring for 12 h. Then the mixture underwent dialysis (MWCO = 50000) to remove excess sodium hyaluronic acid. As a control, **HA@Ru2** were prepared using the same method as mentioned above except the **RuS2 NPs** were replaced with **Ru2** complexes.

The formation of **RuS NPs** and **HA@RuS2 NPs** was characterized by UV-Vis, IR, TEM, DLS and ICP-MS.

Two-photon absorption cross section measurement

The two-photon absorption (TPA) cross section was measured according to previous reported method.[3] Samples in MeOH at a 0.1 mM concentration were placed in fluorometric quartz cuvette at 298K. The experimental fluorescence excitation and detection conditions were conducted with negligible reabsorption processes. The TPA spectra were determined from 790-900 nm. And the cross-section value was calculated at each wavelength according to the equation as follow:

$$\delta_S = \delta_R \cdot \frac{\phi_R C_R I_S n_S}{\phi_S C_S I_R n_R} \quad (1)$$

Where δ is the two-photon absorption cross-section, Φ is the quantum yield, C is the concentration, I is the integrated emission intensity at each wavelength, and n is the refractive index. Subscript 'S' stands for samples, 'R' stands for the reference, rhodamine B.

Electron spin resonance (ESR) assay

The ESR measurements were carried out with a Bruker Model A300 spectrometer at 298K. All ESR measurements were carried out by using the same settings to detect the spin adducts: 20 mW microwave power, 100 G-scan range, and 1 G field modulation. The spin trap 2,2,6,6-tetramethylpiperidine (TEMP for trapping $^1O_2$, 5 mM) was used to verify the formation of $^1O_2$ generated by **Ru1**, **Ru2**, **RuS1 NPs** and **RuS2 NPs** (10 μM) under irradiation.

Cell lines and culture conditions

The human breast cancer cell line (MDA-mB-231) was obtained from Guangzhou Sigene Biological Technology Co. LTD (Guangzhou, China). The cells were incubated in Dulbecco's modified Eagle medium (DMEM, Gibco BRL) supplemented with 10% (v/v) fetal bovine serum (FBS, Gibco BRL) and 100 μg/mL streptomycin, and 100 U/mL penicillin (Gibco BRL) under 100% air at 37°C in a humidified atmosphere.

Quantitative analysis of the content of Ru in cells

The MDA-mB-231 cells were seeded in 10 cm dishes and allowed to grow for 24 h. After removal of medium, **Ru1, Ru2, RuS1 NPs** and **RuS2 NPs** were added into cells and incubated for 2, 4, 6, 8, 12, or 24 h. Then the cells were washed with PBS and harvested by digestion with trypsin. The resulting cell pellets were digested with HNO_3 (60%) and H_2O_2 (20%) for more than 24 h. All the samples were tested by ICP-MS to quantify the ruthenium content.

***In vitro* Ru(II) complexes release from RuS NPs**

Dual triggered Ru(II) complexes release from RuS NPs was determined using dialysis procedure (MWCO = 3500). 1mL of **RuS1 NPs** or **RuS2 NPs** (1 mM) was placed into a dialysis bag under various buffer solutions (50 mL) as follow, ie., (1) PBS (pH 7.4); (2) PBS (pH 7.4) with 10 mM GSH; (3) PBS (pH 5.5); (4) PBS (pH 5.5) with 10 mM GSH. At certain times, 0.5 mL outside buffer solution was taken out and completely digested by 0.5 mL concentrated HNO_3 and 1.0 mL 30% H_2O_2 in room temperature for 24 h. Finally, all samples were diluted to a total 10 mL specimens with Milli Q H_2O and determined by ICP-MS. Quantification was calculated by ruthenium standard curve.

***In vitro* cytotoxicity measurements**

Before experiment **Ru1**, **Ru2**, **RuS1 NPs** and **RuS2 NPs** were first dissolved in DMSO and prepared as a 20 mM stock solution, and the final concentration of DMSO was kept less than 0.5 % (v/v).The MDA-mB-231 cells were seeded in triplicate into 96-well plates for 24 h. **Ru1, Ru2, RuS1 NPs** and **RuS2 NPs** were added in each well and incubated for 6 h. After refreshing with new DMEM medium, the cells were exposed to one-/two-photon irradiation (450 nm, 20 mW, 300 s; 810 nm, 40 mW, 120 s) or incubated without any treatment. After incubation for another 24 h, 3-(4,5-dimethyl-2-thiazolyl)-2,5-diphenyl-2-H-tetrazolium bromide (MTT) was added into each well for another 4 h incubation. Finally, the media were discarded and 150 μL of DMSO was added. The optical density at 595 nm of each well was measured by microplate reader. Data were represented as the means ± standard deviation (n = 3).

For live/dead cell detecting, MDA-mB-231 cells were seeded the same manner as above. Pre-treated with or without α-lipoic acid (LPA, a GSH synthesis enhancer, 500 μM), the cells were incubated with **RuS1 NPs** and **RuS2 NPs** for 6 h and then exposed to two-photon irradiation (810 nm, 40 mW, 120 s). Calcein-AM (λ_{ex} = 488 nm, λ_{em} = 500-520 nm) and ethidium (λ_{ex} = 543 nm, λ_{em} = 590-630 nm) were used to stain the cells for another 30 min. Cell imaging was performed using a Zeiss LSM 810 NLO confocal microscope.

One- and two-photon cellular imaging and subcellular organelle colocalization

The MDA-mB-231 cells were seeded in confocal microscopy dishes and incubated for at least 24 h. Then **Ru1**, **Ru2**, **RuS1 NPs** and **RuS2 NPs** were added for 6 h incubation. The cells were washed with PBS three times and then imaged in a Zeiss LSM 810 NLO confocal microscope (63xoil/NA 1.4 oil immersion objective). **Ru1** and **RuS1 NPs** ($\lambda_{one\text{-}photon,\ ex}$ = 458 nm, $\lambda_{two\text{-}photon,\ ex}$ = 800 nm, λ_{em} = 580-610 nm). **Ru2** and **RuS2 NPs** ($\lambda_{one\text{-}photon,\ ex}$ = 458 nm, $\lambda_{two\text{-}photon,\ ex}$ = 810 nm, λ_{em} = 590-620 nm).

For subcellular organelle co-localization analysis, Lyso-Tracker Green (LTG, 50 nM) or Mito-Tracker Green (MTG, 50 nM) were added for another 30 min incubation after **Ru1, Ru2, RuS1 NPs** and **RuS2 NPs** treatment. **LTG** or **MTG** (λ_{ex} = 488 nm, λ_{em} = 515-535 nm)

Two-photon imaging of multicellular tumor spheroid

Three-dimensional multicellular tumor spheroids (MCTSs) were formed in agarose-based 96-well plates according to the previously reported method.[4] 50 μL of a 2.5 x 10^4 MDA-mB-231 cells/mL trypsin-digested cells were seeded onto agarose-based (1.5% (w/v) in PBS) 96-well plates. The cells were able to aggregate spontaneously, resulting in the formation of MCTSs with diameters varying from 300-400 μm after 96 h. Pre-incubation with or without genistein (Gen, 200 μM), MCTSs were treated with **RuS1 NPs** and **RuS2 NPs** for 6 h. Then the cell spheroids were gently washed twice with PBS and imaged by confocal microscopy (10x/NA objective).

Bio-TEM imaging analysis

MDA-mB-231 cells treated with **RuS1 NPs** or **RuS2 NPs** (10 μM) for 2 h, 4 h and 6 h, were washed with PBS, trypsinized, and collected by centrifugation. For bio-TEM imaging analysis, cells were fixed in 0.1 M PBS containing 2.5% glutaraldehyde and 4% paraformaldehyde for 1 h, rinsed with distilled water, stained with 0.5% uranyl acetate for 1 h, dehydrated in a graded series of EtOH (30, 60, 70, 90 and 100%), and embedded in epoxy resin. The resin was polymerized at 60 °C for 48 h. Ultrathin sections (50-75 nm) obtained with a LKB

ultramicrotome were stained with 2% aqueous uranyl acetate and 2% aqueous lead citrate.

***In vitro* ROS generation assay**

The $^1O_2$ production capacity of **Ru1**, **Ru2**, **RuS1 NPs** and **RuS2 NPs** in cells was evaluated using flow cytometry method. Cells were seeded into 6-well plates for 24 h. **Ru1**, **Ru2**, **RuS1 NPs** and **RuS2 NPs** (10 μM) were then added for a 6 h incubation. Then the medium was removed and cells were washed with fresh medium. 1.0 mL fresh medium containing DCFH-DA (20 μM) was added into the cells. After incubation for another 30 min, the cells were then exposed to irradiation (450 nm, 20 mW, 300 s). In the control group, the cells were only treated with DCFH-DA and irradiation. Then, the cells were washed with PBS and collected by trypsin-digestion to obtain a suspension solution in cold PBS. Finally, the data were recorded by flow cytometry. For each cell population, 10000 live cells were analyzed.

Flow cytometric analysis of cell apoptosis

The MDA-mB-231 cells were seeded into 6-well plates the same manner as above. **Ru1**, **Ru2**, **RuS1 NPs** and **RuS2 NPs** (10 μM) were added for a 6 h incubation. The cells were washed with PBS three times and then exposed to irradiation (450 nm, 20 mW, 300 s). After 24 h incubation, the cells were trypsinized, collected and stained with Annexin V/PI and the data were recorded by flow cytometry. The non-exposed cells were set as control groups. For each cell population, 10000 live cells were analyzed.

***In vivo* imaging and *in vivo* two-photon PDT**

6-8 weeks age nu/nu female mice were purchased from Guangzhou Sigene Biological Technology Co. LTD. This study was performed with the approval of the Experimental Animal Manage Committee (EAMC) of Guangdong Pharmaceutical University (certificate number: GDPULAC2020249). The animal experiments were commissioned by Guangzhou Sigene Biological Technology Co. LTD and treated as the guidelines of EAMC. 6 x 10^6 MDA-mB-231 cells in a suspension in 150 μL Matrigel (Corning) and saline (1:1, v/v) were subcutaneously (s.c.) injected into the nude mice. When the tumor volumes of the mice reached approximately 100 mm^3, the MDA-mB-231 tumor xenograft model was established.

For the *in vivo* imaging, MDA-mB-231-bearing mice were intravenously (i.v.) injected with saline, **RuS2 NPs** and **HA@RuS2 NPs**, and then imaged with an *in vivo* imaging system (IVIS Lumina XRMS Series III) after 0.5, 2, 4, 6, 12 and 24 h. Then mice were sacrificed to excise tumors and organs, and the *ex vivo* images were obtained using IVIS spectrum.

For two-photon PDT, the MDA-mB-231 tumor-bearing nude mice were separated into 6 groups stochastically.

Group 1: Intravenously (i.v.) injected with **Saline**;

Group 2: Intravenously (i.v.) injected with **Saline** 6 h later, the mice were treated with 810 nm laser (50 mW, 1 kHz, pulse width 35 fs, 5 s/mm);

Group 3: Intravenously (i.v.) injected with **RuS2 NPs** (10 mg/kg based on Ru(II) complex);

Group 4: Intravenously (i.v.) injected with **RuS2 NPs** (10 mg/kg). 6 h later, the mice were treated with 810 nm laser (50 mW, 1 kHz, pulse width 35 fs, 5 s/mm);

Group 5: Intravenously(i.v.) injected with **HA@RuS2 NPs**;

Group 6: Intravenously(i.v.) injected with **HA@RuS2 NPs** 6 h later, the mice were treated with 810 nm laser (50

mW, 1 kHz, pulse width 35 fs, 5 s/mm).

The mice were then observed for the next two weeks. Their body weights and tumor volumes were measured every two days. The tumor volume was calculated by the equation as follow:

$$volume = \frac{Length \times Width^2}{2} \tag{2}$$

All mice were sacrificed at the end of two-photon PDT. Tumors were collected and dissected from remaining tumor-bearing mice. The major organs (heart, liver, spleen, lung, kidney) were resected and immersed in 4% paraformaldehyde at 4°C. For morphological studies, 6 μm sections were acquired from paraffin-embedded samples, processed according to the standard procedures for inclusion, and rehydrated (xylene, alcohol, water). The sections were stained with hematoxylin-eosin (H&E) and observed with a Carl Zeis Axio Imager Z2 microscope.

Results and Discussion

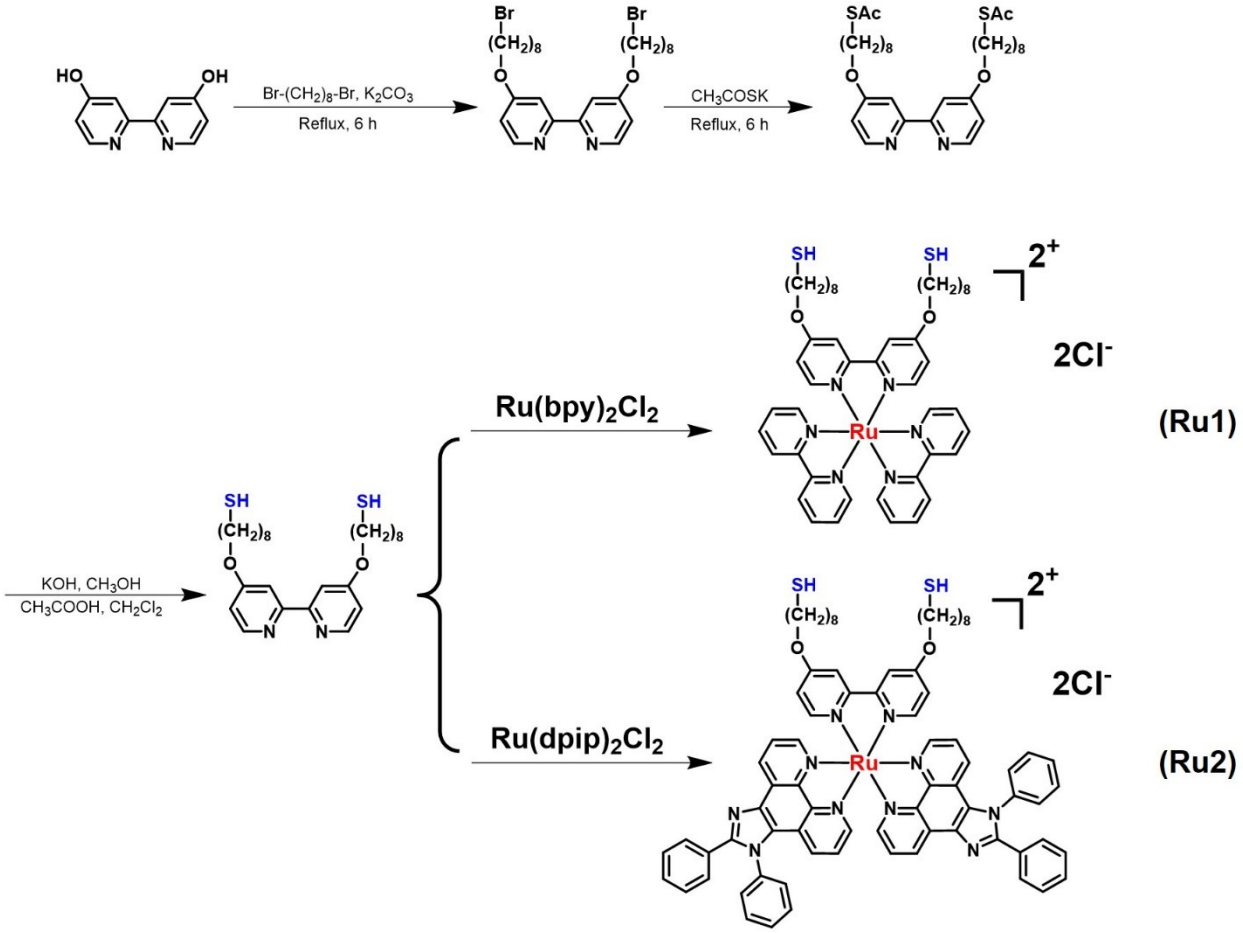

Scheme S1. Synthetic routes to **Ru1** and **Ru2**

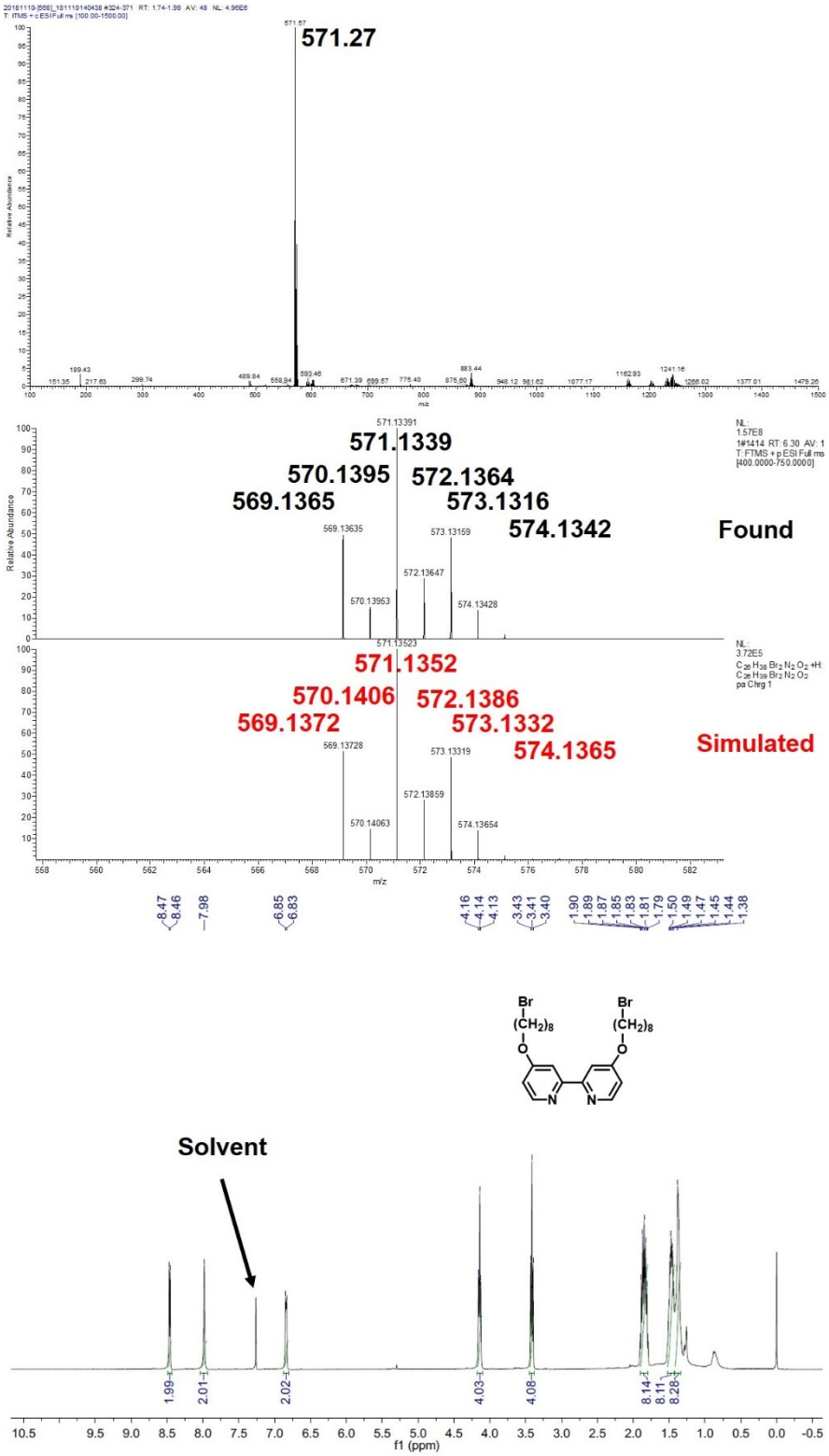

Figure S1. ESI-MS, HR-MS and ^{1}H NMR spectra (400 MHz, $CDCl_3$) of **bpy-2Br**.

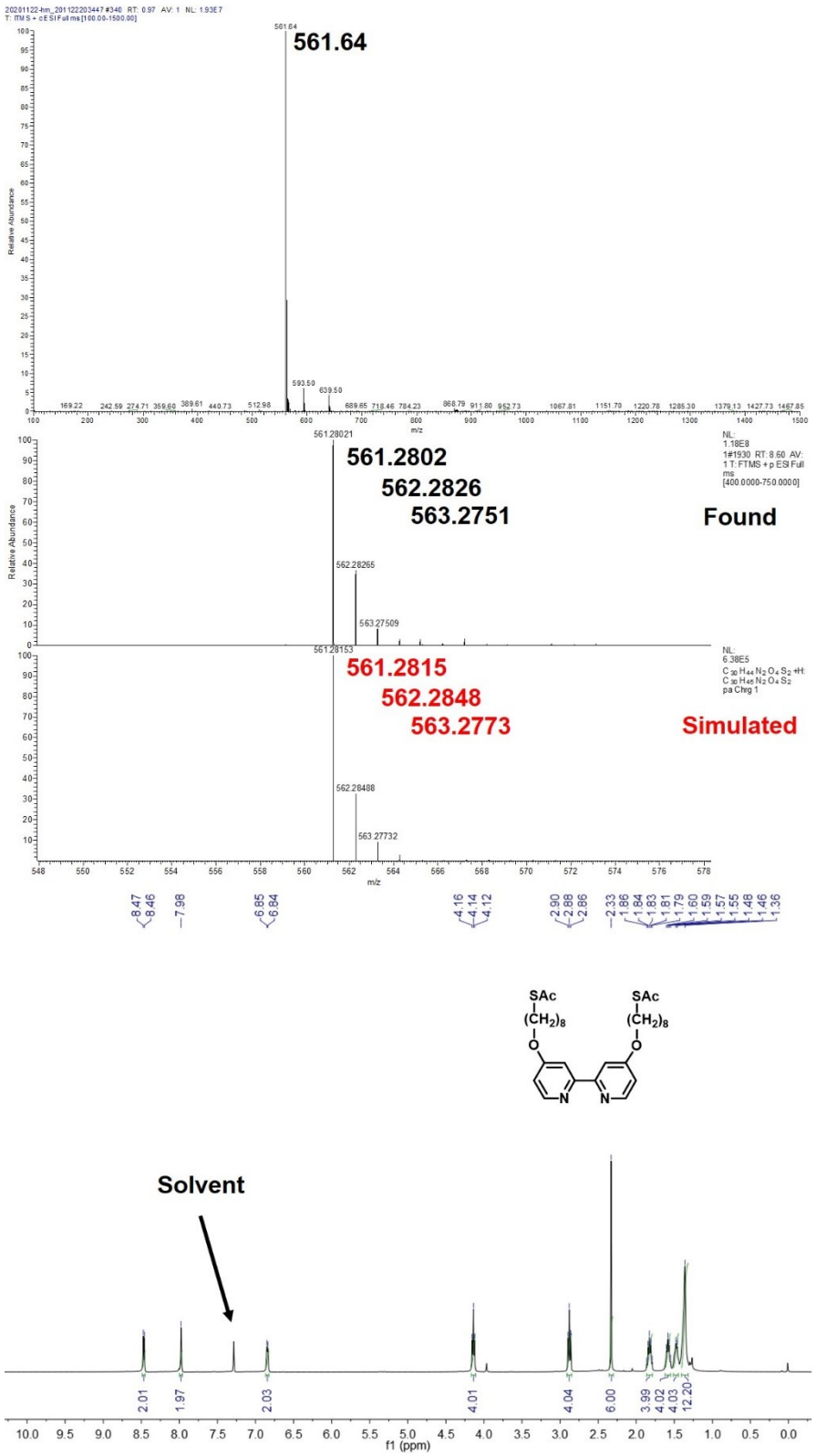

Figure S2. ESI-MS, HR-MS and ^{1}H NMR spectra (400 MHz, $CDCl_3$) of **bpy-2SAc**.

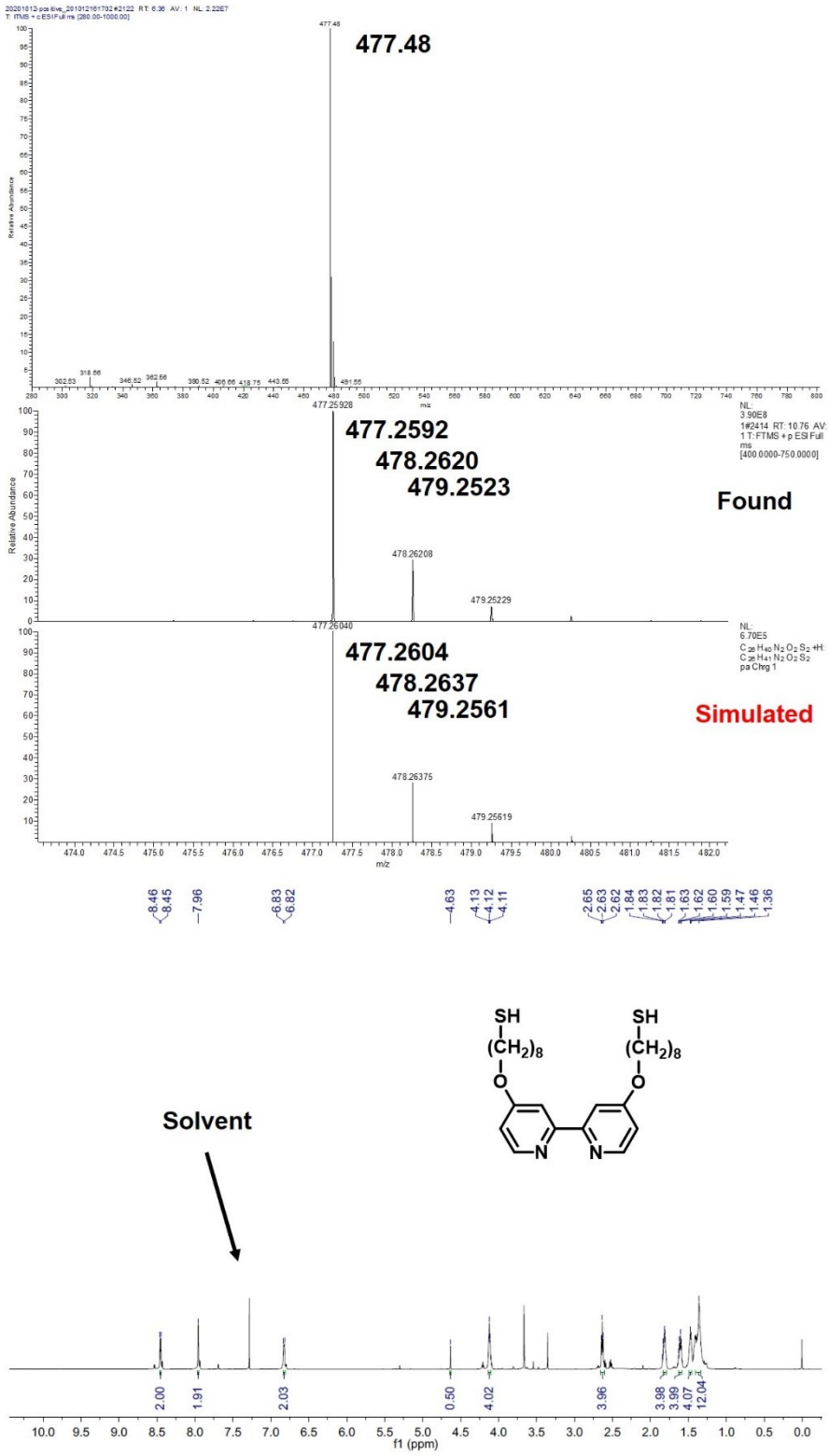

Figure S3. ESI-MS, HR-MS and ^{1}H NMR spectra (400 MHz, $CDCl_3$) of **bpy-2SH**.

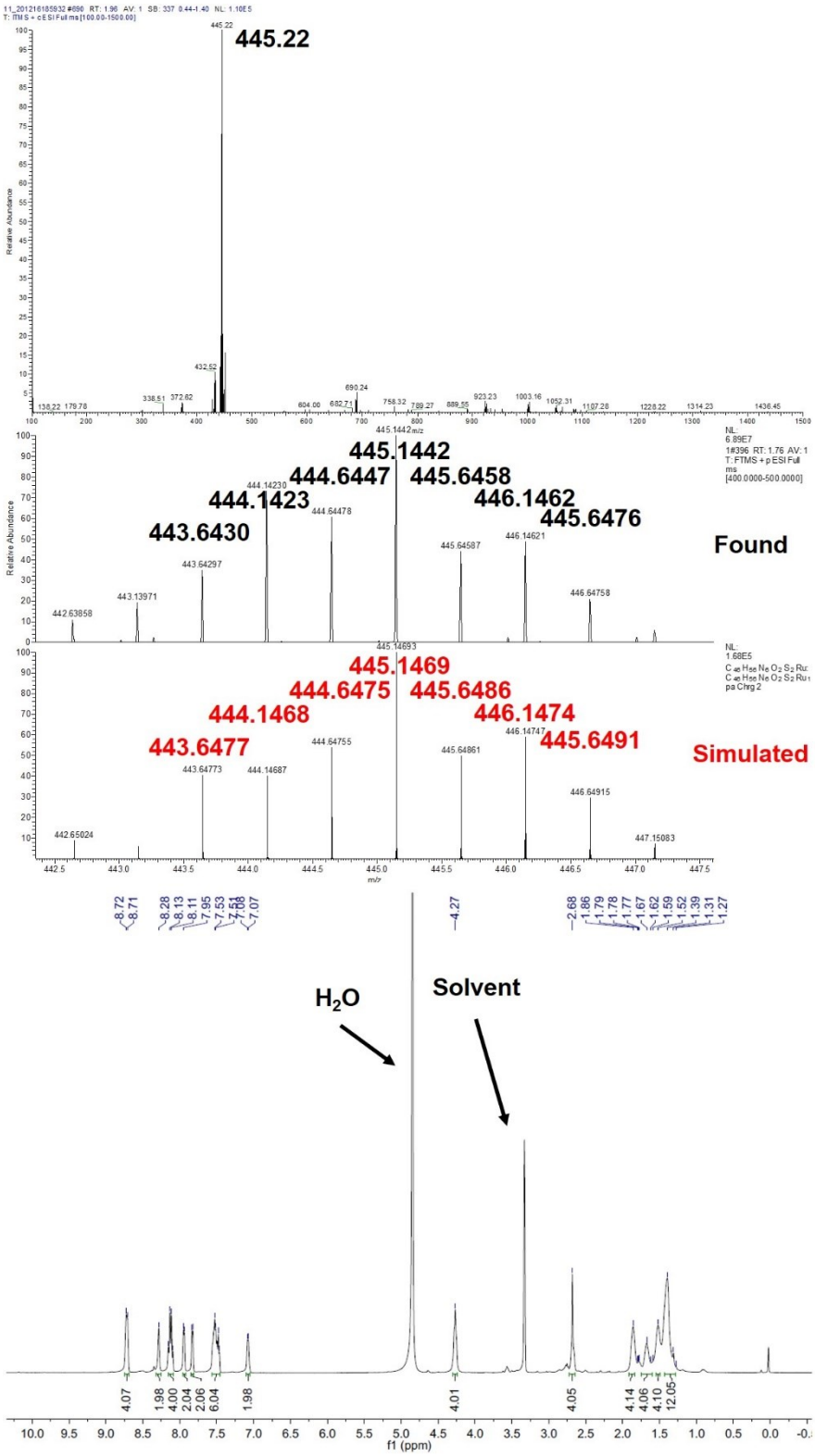

Figure S4. ESI-MS, HR-MS and ^{1}H NMR spectra (400 MHz, CD_3OD) of **Ru1**.

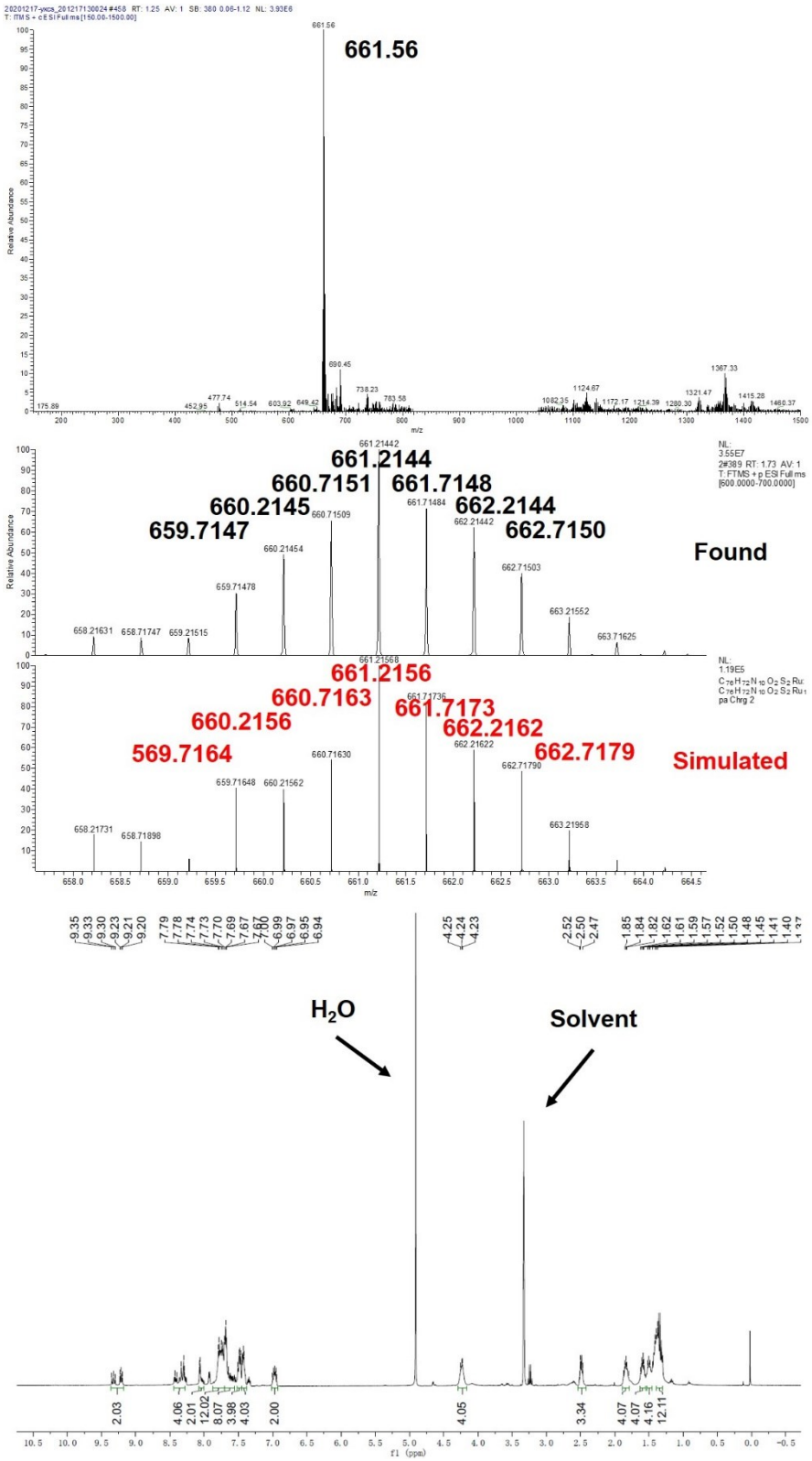

Figure S5. ESI-MS, HR-MS and ^{1}H NMR spectra (400 MHz, CD_3OD) of **Ru2**.

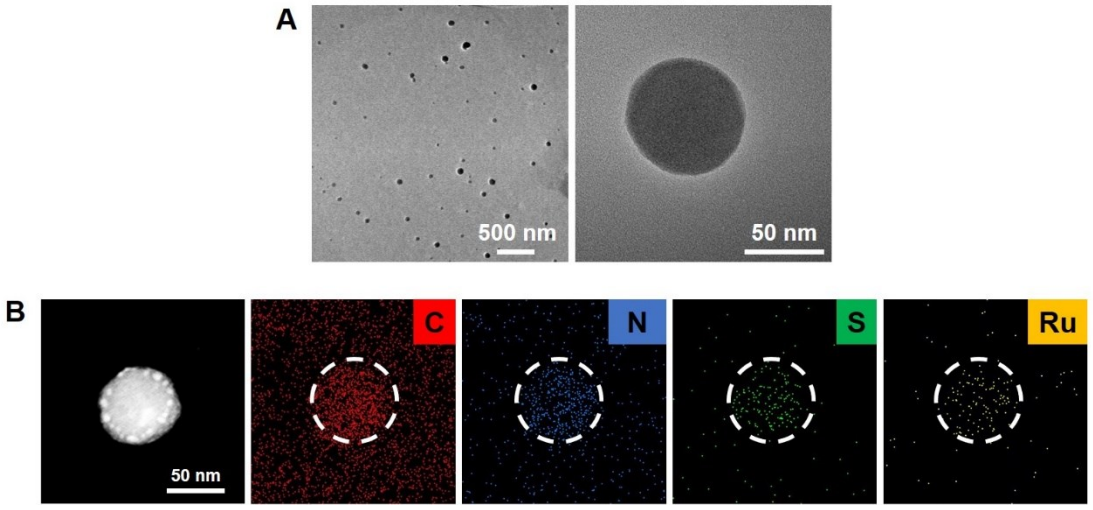

Figure S6. A) TEM image and High-resolution TEM image of **RuS1 NPs**. B) Highly-magnified HAADF-STEM image and elemental mapping of **RuS1 NPs**.

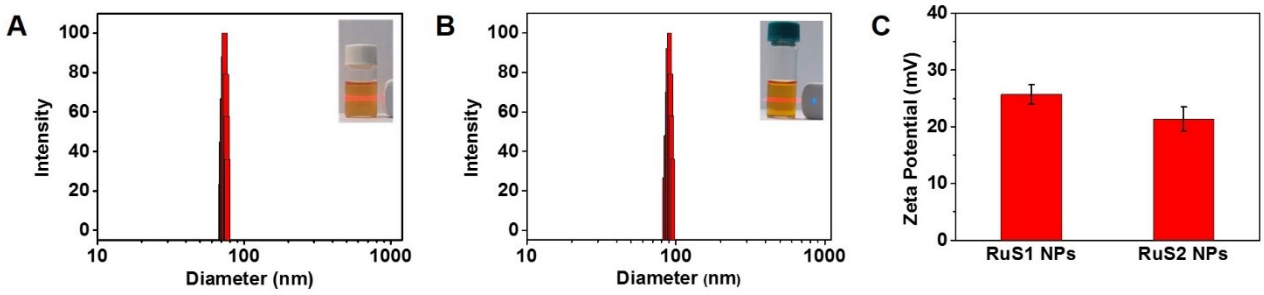

Figure S7. Hydrodynamic diameter of A) **RuS1 NPs** and B) **RuS2 NPs**. Inset: Photograph of **RuS NPs** under irradiation. C) Zeta potential data of **RuS1 NPs** and **RuS2 NPs**.

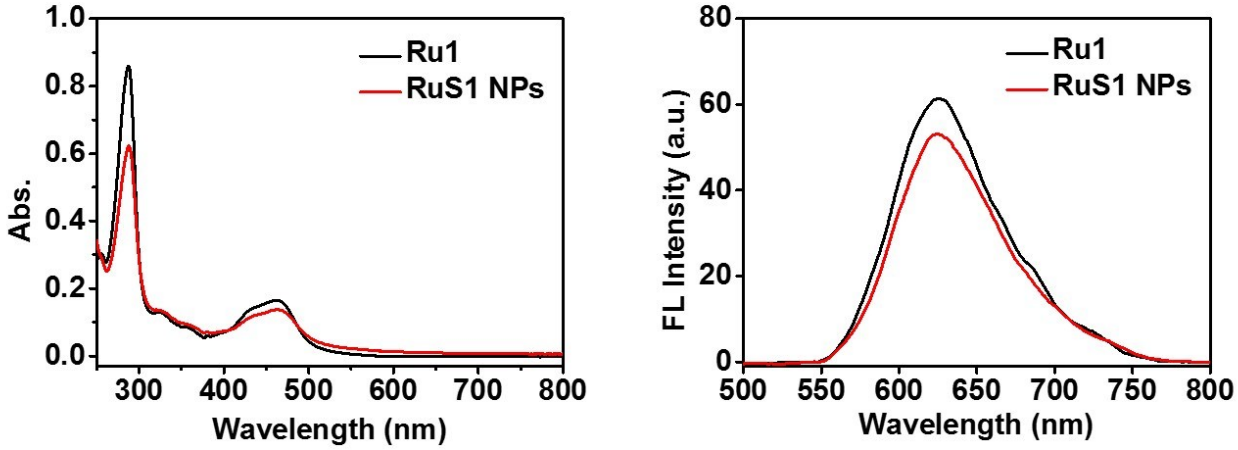

Figure S8. UV-Vis absorption and emission spectra of **RuS1** and **RuS1 NPs**. (λ_{ex} = 450 nm, for emission spectra)

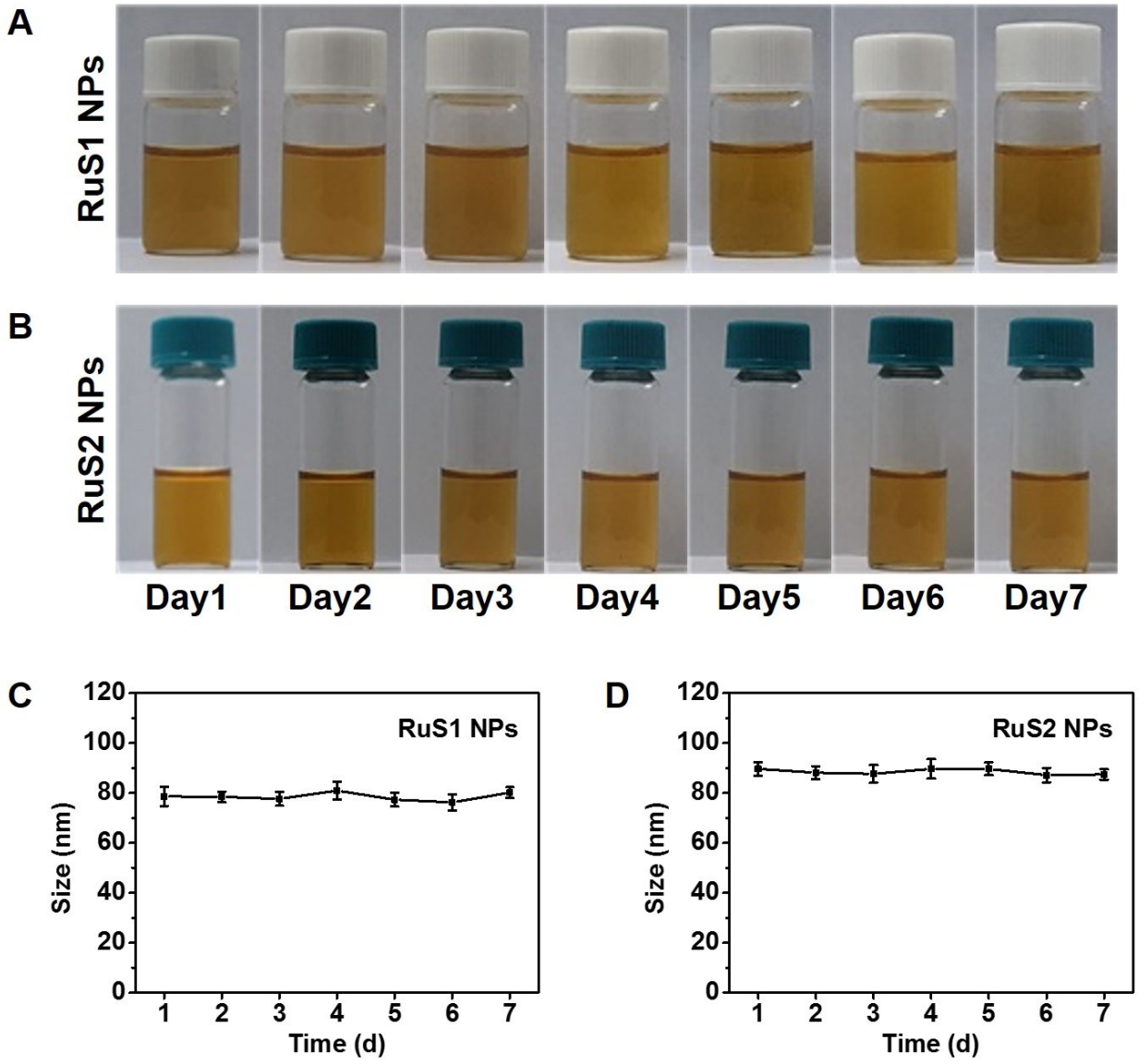

Figure S9. Stability test of **RuS NPs**. Photography of A) **RuS1 NPs** and B) **RuS2 NPs** in PBS buffer (pH = 7.4) stored at room temperature for 7 days. Hydrodynamic diameter changes of C) **RuS1 NPs** and D) **RuS2 NPs** within 7 days.

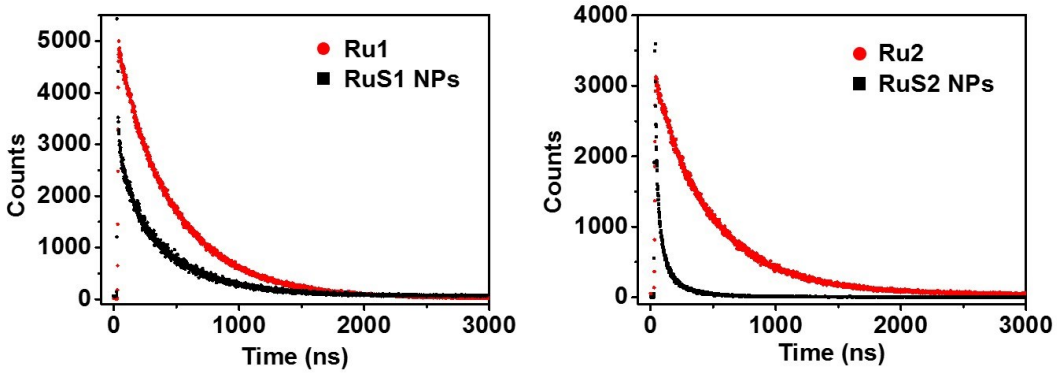

Figure S10. The lifetime decay curve of **Ru1**, **Ru2**, **RuS1 NPs** and **RuS2 NPs**.

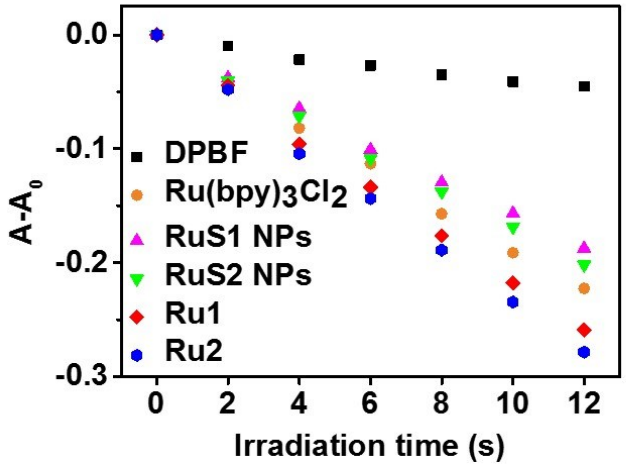

Figure S11. Plots of the relative emission change of DPBF at 410 nm versus irradiation time in the presence of **Ru1**, **Ru2**, **RuS1 NPs** and **RuS2 NPs** in CH_3OH. The irradiation wavelength is 450 nm.

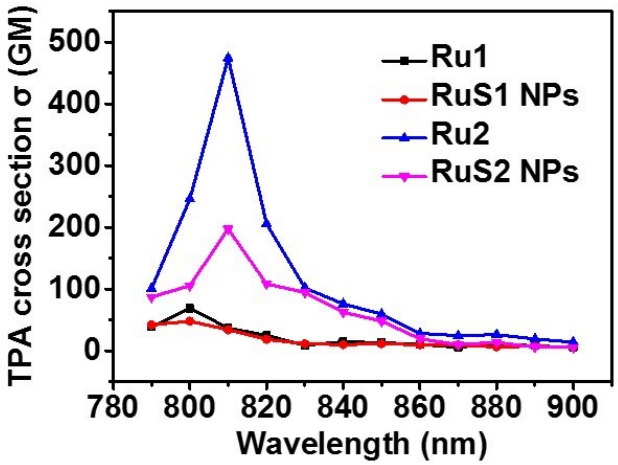

Figure S12. Two-photon absorption cross sections of **Ru1**, **Ru2**, **RuS1 NPs** and **RuS2 NPs** at different excitation wavelengths from 790 to 900 nm in CH_3OH.

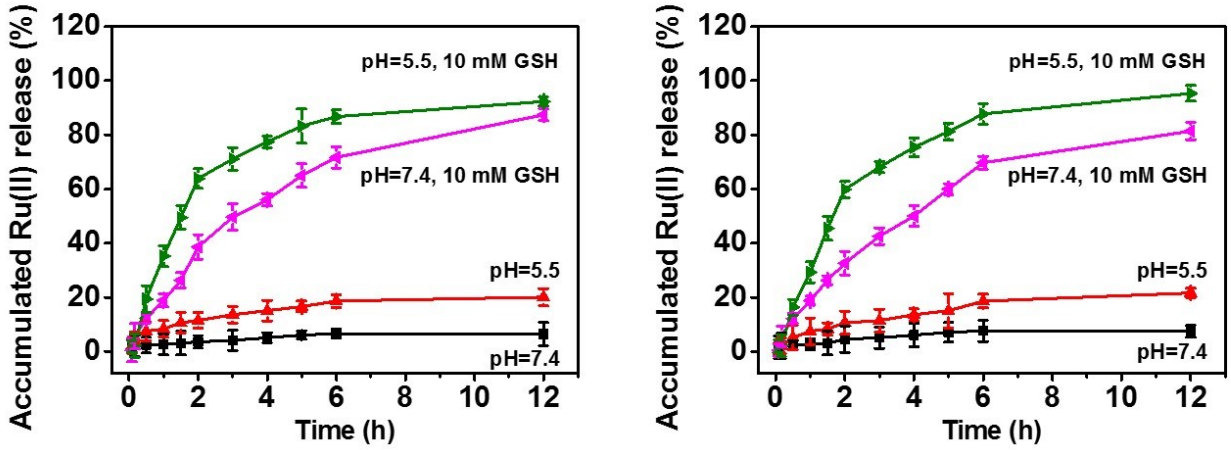

Figure S13. *In vitro* Ru(II) complexes release of **RuS1 NPs** (left) and **RuS2 NPs** (right) in different buffer solutions (**RuS1 NPs** and **RuS2 NPs**, 1 mM).

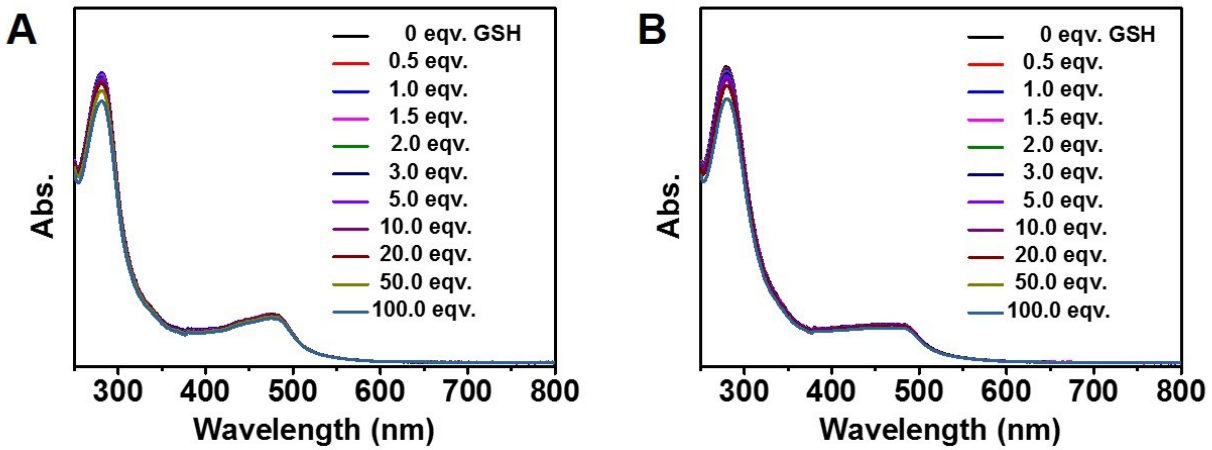

Figure S14. UV-vis absorption spectra of A) **RuS1 NPs** and B) **RuS2 NPs** (10 μM) with addition of increasing concentrations of GSH equivalent to Ru(II) in PBS buffer.

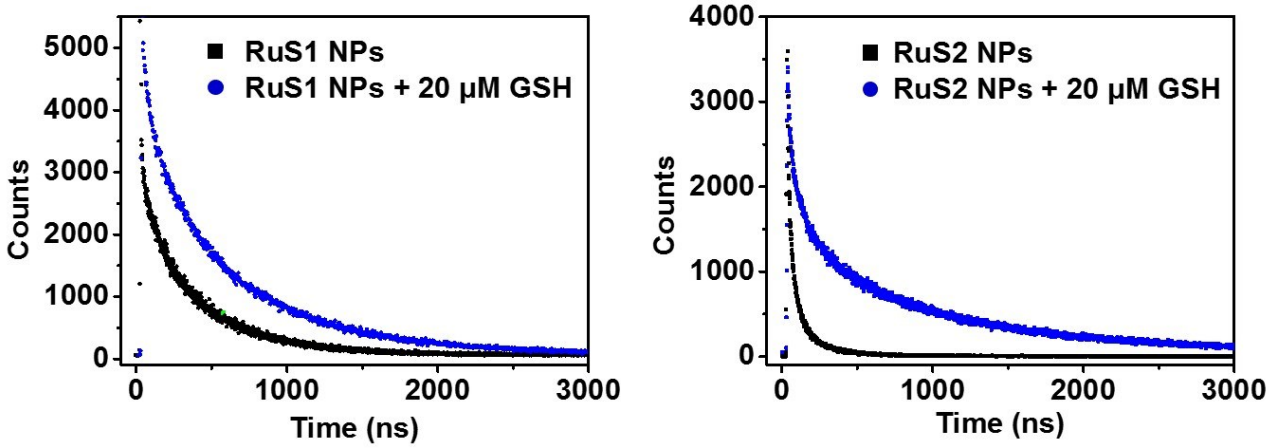

Figure S15. The lifetime decay curves of **RuS1 NPs** and **RuS2 NPs** (10 μM) with and without GSH.

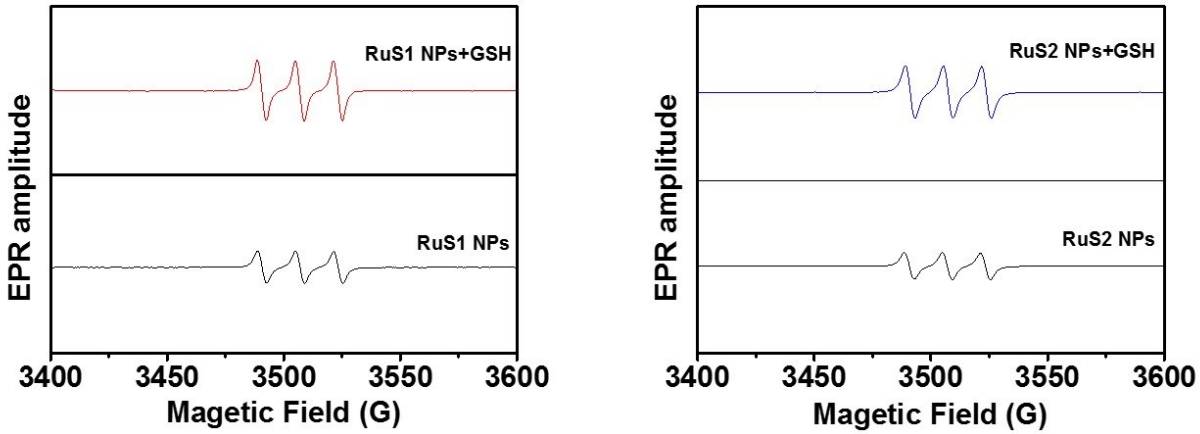

Figure S16. The EPR signal of **RuS1 NPs** and **RuS2 NPs** (10 μM) with or without the addition of GSH (20 μM) upon 450 nm irradiation.

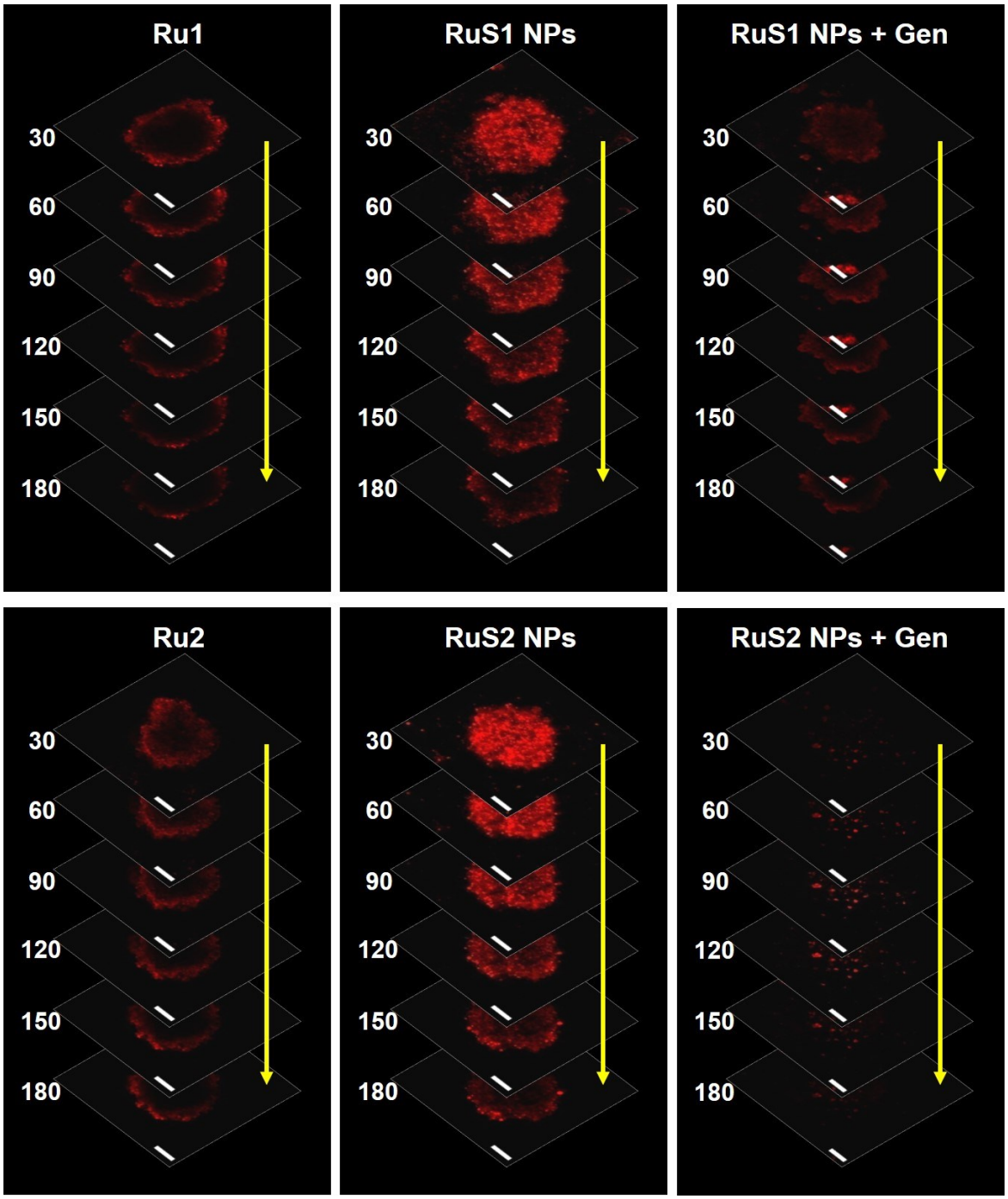

Figure S17. Z-stack images of MDA-mB-231 3D multicellular spheroids incubated with **Ru1**, **Ru2**, **RuS1 NPs** and **RuS2 NPs** (10 μM) pre-treated with or without Gen for 6 h with intervals of 30 μm. $\lambda_{ex\text{-}TPM}$ = 810 nm, λ_{em} = 620 nm. The images were taken under 10 x objective. Scale bar: 100 μm.

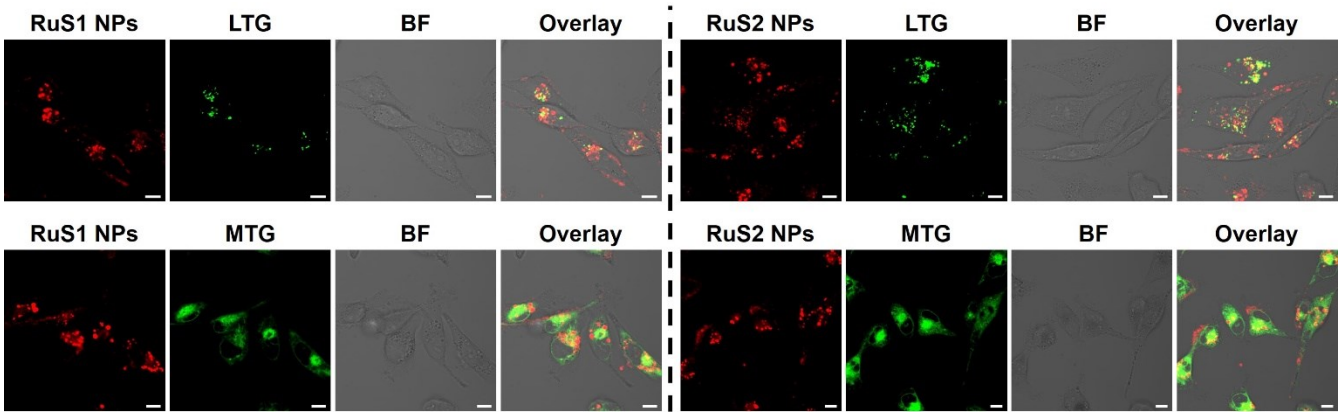

Figure S18. Confocal images of MDA-mB-231 cells co-labelled with **RuS1 NPs** or **RuS2 NPs** and LTG (50 nM) or MTG (50 nM). Scale bar: 10 μm.

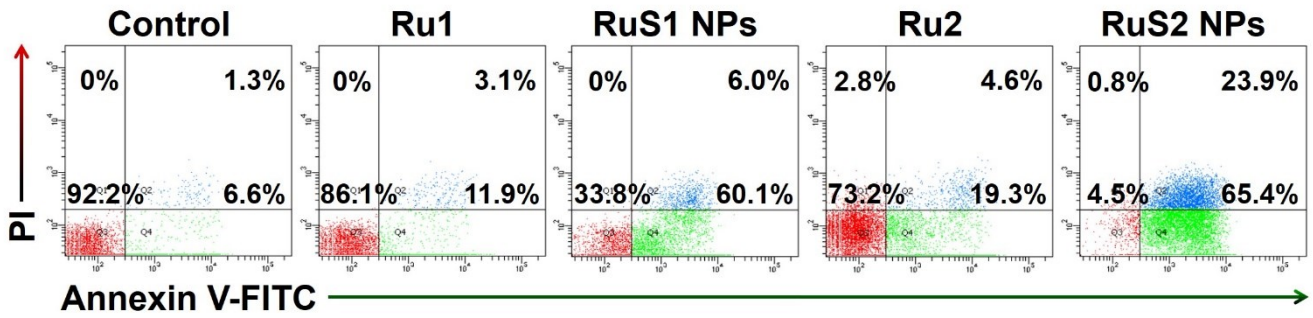

Figure S19. Flow cytometric analysis of Annexin V-FITC/propidium iodide (PI) stained MDA-mB-231 cells incubated with **Ru1, Ru2, RuS1 NPs** and **RuS2 NPs** (10 μM) for 6 h upon irradiation (450 nm, 20 mW/cm^2, 300 s).

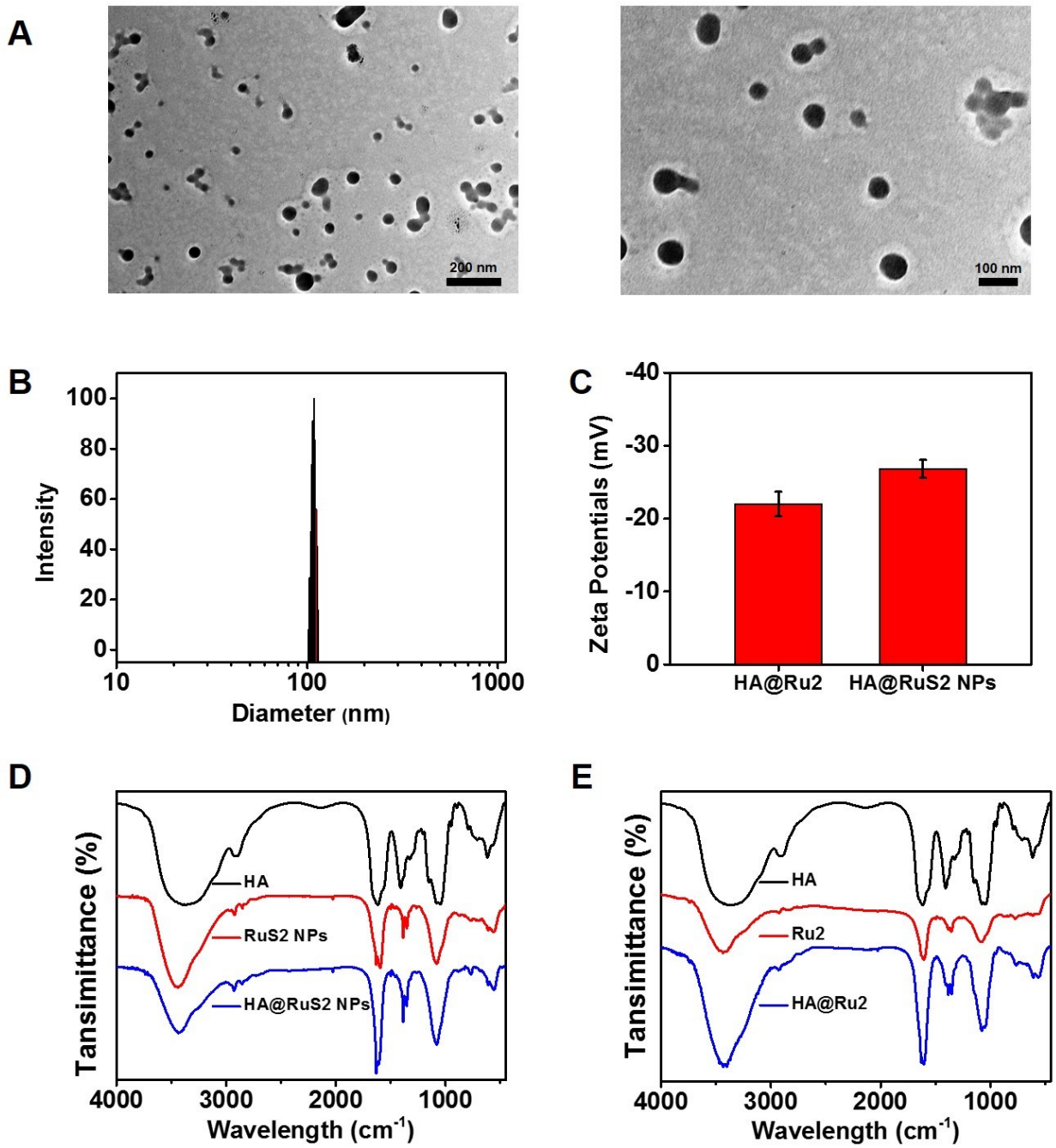

Figure S20. A) TEM images and B) Hydrodynamic diameter of **HA@RuS2 NPs**. C) Zeta potentials measurement of **HA@Ru2** and **HA@RuS2 NPs**. D) FT-IR spectra of hyaluronic acid (HA), **RuS2 NPs** and **HA@RuS2 NPs**. E) FT-IR spectra of hyaluronic acid (HA), **Ru2** and **HA@Ru2**.

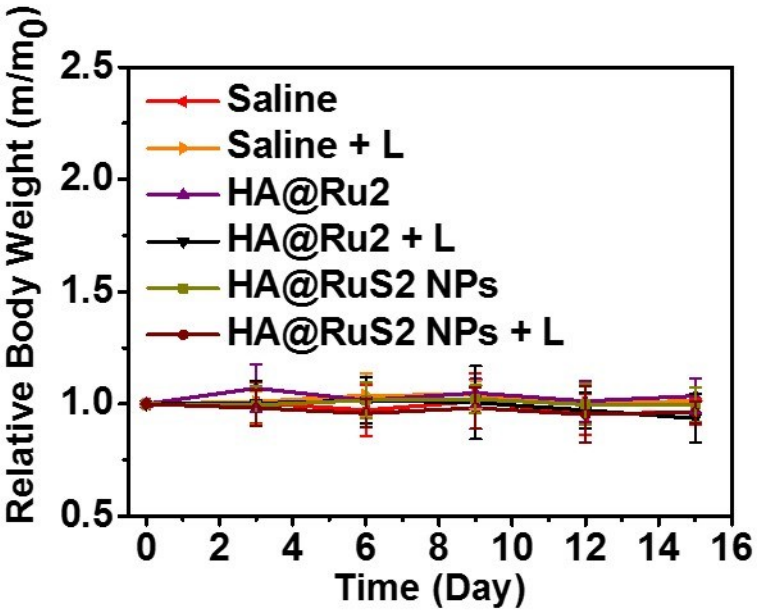

Figure S21. Body weight of mice after various treatments. Mice were received i.v. injection of saline, **HA@Ru2** and **HA@RuS2 NPs** (0.01 mmol/kg Ru(II)) with or without 810 nm laser irradiation.

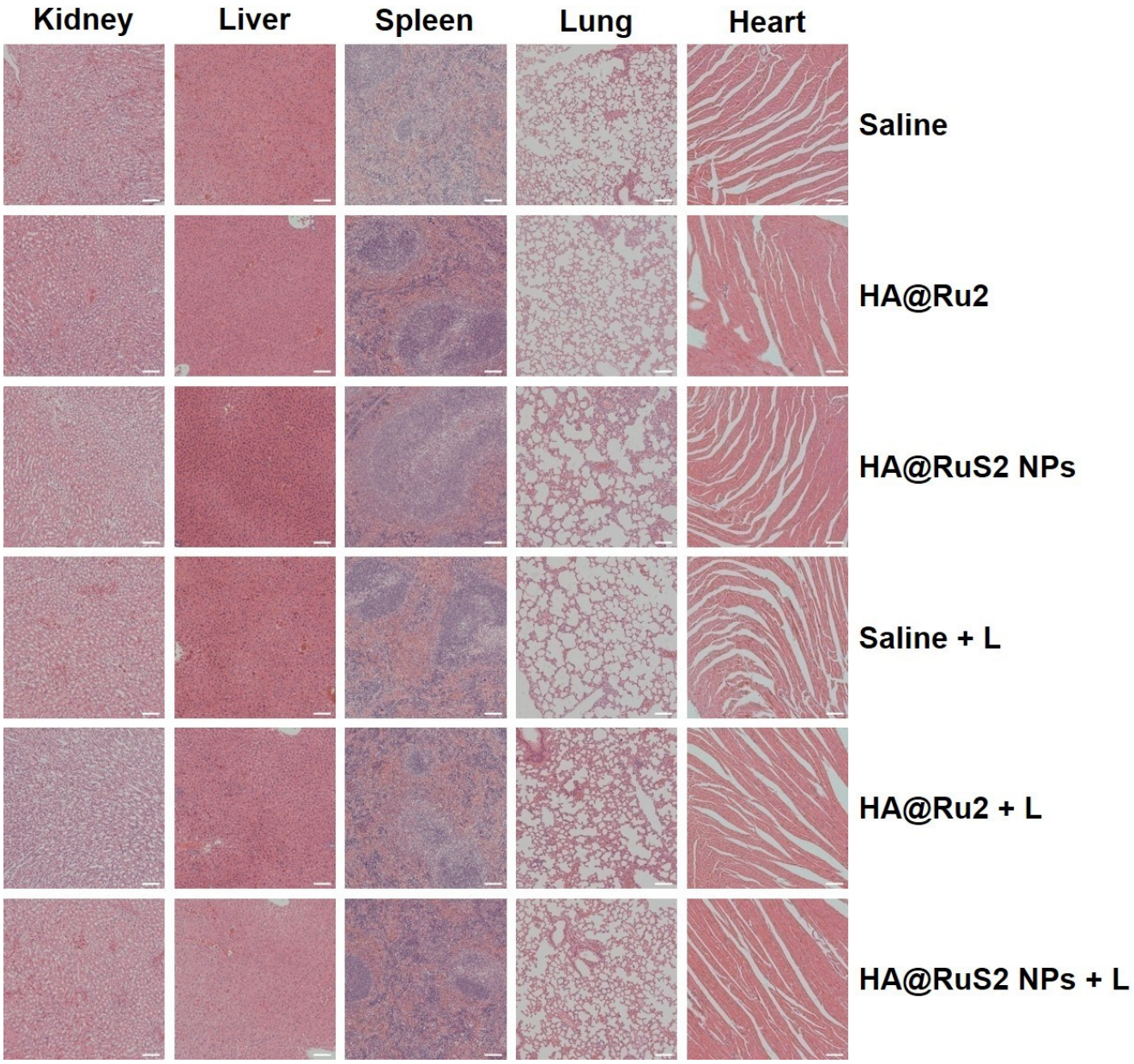

Figure S22. Histological examination of major organs (kidney, liver, spleen, lung and heart) after various treatments. Mice were received i.v. injection of saline, **HA@Ru2** and **HA@RuS2 NPs** (0.01 mmol/kg Ru(II)) with or without 810 nm laser irradiation. Sections for light microscopy were stained with hematoxylin-eosin (H&E). Magnification was 200×. Scale bar: 50 μm.

References

1. B. P. Sullivan, D. J. Salmon and T. J. Meyer, *Inorg. Chem.*, 1978, **17**, 3334.
2. P. Zhang, H. Huang, Y. Chen, J. Wang, L. Ji and H. Chao, *Biomaterials*, 2015, **53**, 522.
3. C. Xu and W. W. Webb, *J. Opt. Soc. Am. B*, 1996, **13**, 481.
4. H. Huang, P. Zhang, H. Chen, L. Ji and Chao, H. *Chem. Eur. J.*, 2014, **21**, 715.